

Li₂MnCl₄ single crystal: a candidate for novel red-emitting neutron scintillator – Supporting information.

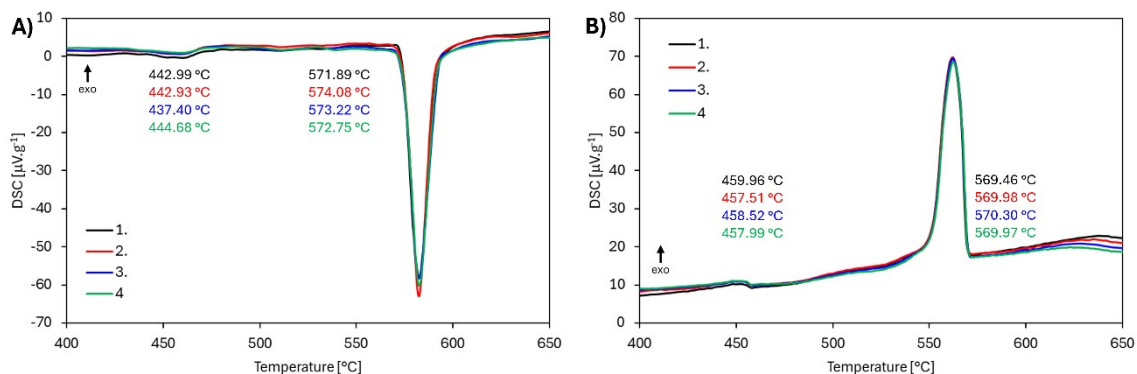


Fig. 1: DSC measurement of the undoped Li₂MnCl₄ sealed in quartz ampoules A) heating curve B) cooling curve. The values of onset temperatures are in separate windows.

Fitting of absorption spectra

The first derivative of the undoped Li₂MnCl₄ absorption spectra was fitted assuming gaussian shaped bands using non-linear least squares. The following formula to fit the band shape:

$$\frac{dA}{dE} a' e^{-\frac{(E-b)^2}{c}} = -\frac{2a'(E-b)}{c} e^{-\frac{(E-b)^2}{c}} = \frac{a(E-b)}{c} e^{-\frac{(E-b)^2}{c}},$$

where a' , a , b , and c are fitting coefficients, E is energy, and A is absorbance. Therefore, the overall fitting function used was:

$$A(E) = d + \sum_{i=1}^6 \frac{a_i(E-b_i)}{c_i} e^{-\frac{(E-b_i)^2}{c_i}},$$

where d is a constant background. The results of the fitting procedure are listed in table S1.

Table S1: Coefficients of the fitting procedure with 95 % confidence intervals.

Coefficient	Value	Lower bound	Upper bound
a1	-0.00504	-0.005207	-0.004872
a2	-0.00342	-0.003642	-0.003207
a3	-0.00195	-0.002105	-0.001798
a4	-0.00029	-0.0003839	-0.0001982
a5	-0.00079	-0.0005855	-0.001003
a6	-0.00099	-0.000819	-0.001157
b1	3.495	3.494	3.496
b2	3.358	3.355	3.36
b3	2.948	2.946	2.95
b4	2.927	2.925	2.929
b5	2.755	2.741	2.77
b6	2.358	2.348	2.368
c1	0.001954	0.001859	0.002049
c2	0.00678	0.006138	0.007422
c3	0.002207	0.001963	0.00245
c4	0.000195	0.0001096	0.0002808
c5	0.01245	0.007537	0.01736
c6	0.01286	0.009464	0.01626
d	-0.002	-0.002216	-0.001784

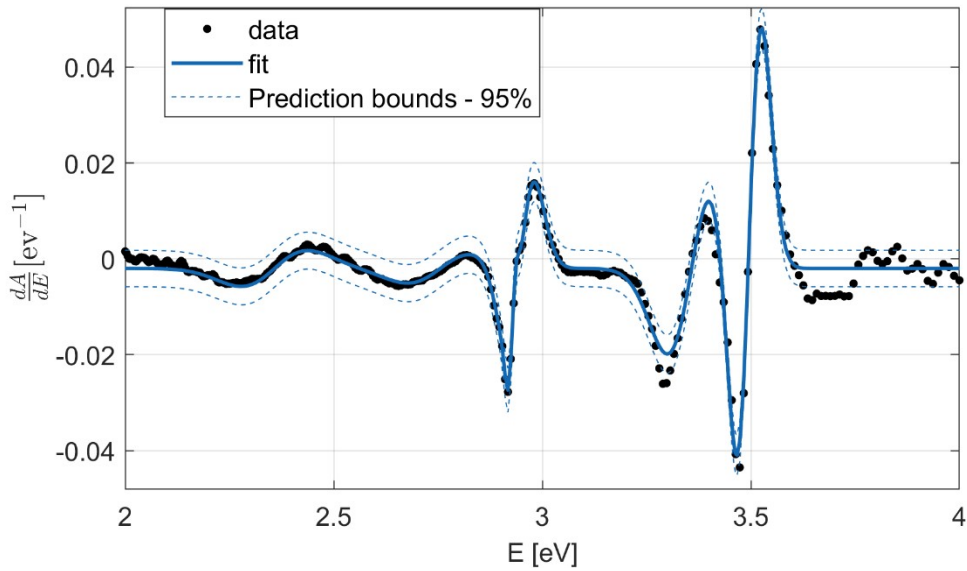


Fig S2: Fitting of the first derivative of absorption spectrum of the undoped Li_2MnCl_4 with six gaussian components. The dashed line shows 95 % prediction bounds.

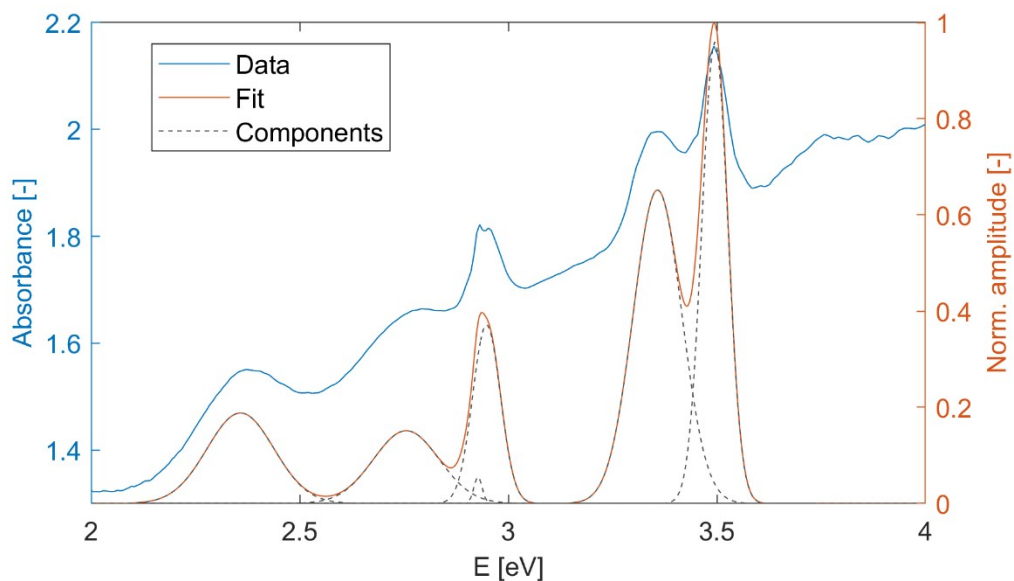


Fig S3: Comparison between the measured absorption spectrum and normalized spectrum reconstructed from the first derivative fitting.

Tab. S2: Position of the absorption bands resulting from the fitting procedure with assigned transitions, ratios between transition energies from absorption spectra E_i/E_1 (exp.) and from Tanabe-Sugano diagram E_i/E_1 (TS) at $D_q/B = 9.1$, corresponding values of E/B and calculated Racah parameter B .

Transition	Band max. [nm]	Band max. [eV]	E_i/E_1 (exp.) [-]	E_i/E_1 (TS) [-]	E/B [-]	B [cm^{-1}]
${}^6A_{1g} \rightarrow {}^4T_{1g} ({}^4G)$	526	2.36	1.00	1.00	26.3	723
${}^6A_{1g} \rightarrow {}^4T_{2g} ({}^4G)$	450	2.76	1.17	1.16	30.4	731
${}^6A_{1g} \rightarrow {}^4A_{1g}, {}^4E_g ({}^4G)$	422	2.94	1.25	1.23	32.4	731
${}^6A_{1g} \rightarrow {}^4T_{2g} ({}^4D)$	369	3.36	1.42	1.42	37.4	725
${}^6A_{1g} \rightarrow {}^4E_g ({}^4D)$	355	3.50	1.48	1.50	39.4	716

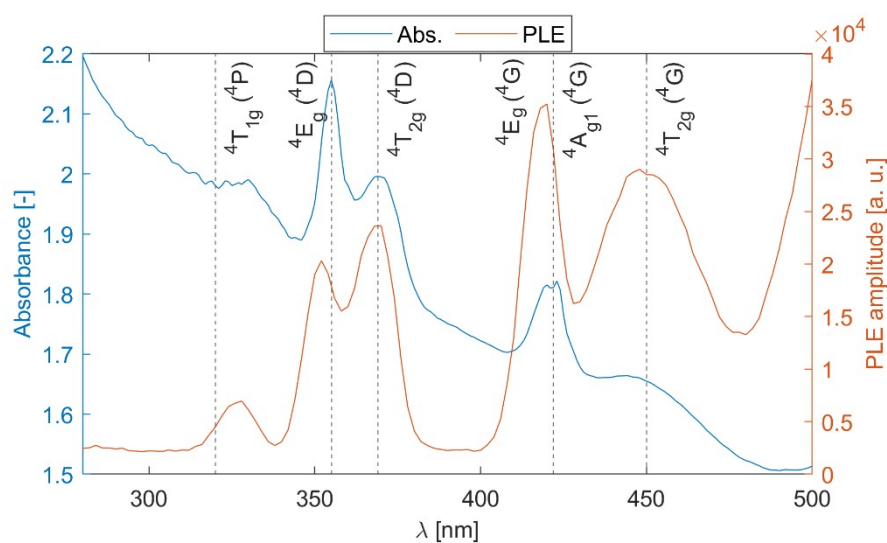


Fig. S4: Comparison of absorption and PLE (em. 620 nm) spectra with band assignment for the undoped Li_2MnCl_4 . The position of the ${}^6\text{A}_{1g} \rightarrow {}^4\text{T}_{1g} ({}^4\text{P})$ transition was determined from the d^5 TS diagram at $D_q/B = 9.1$.

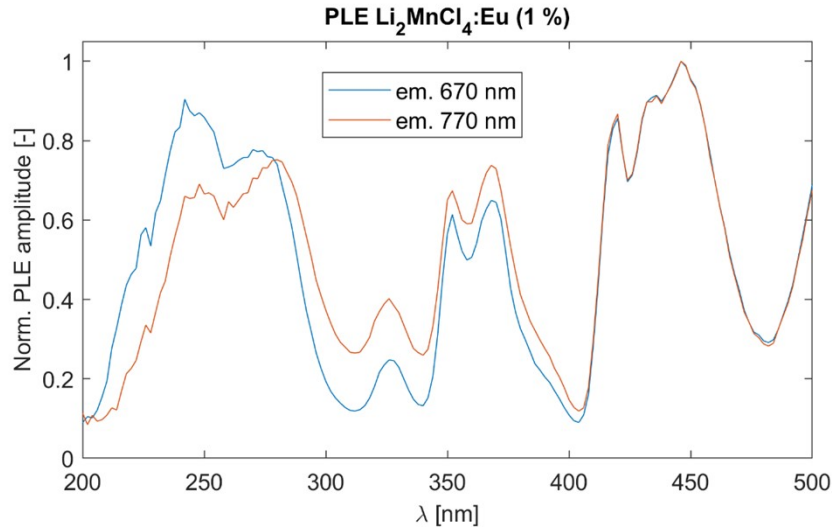


Fig. S5: Normalized PLE spectra of $\text{Li}_2\text{MnCl}_4:\text{Eu}$ for $\lambda_{\text{em}} = 670, 770$ nm.

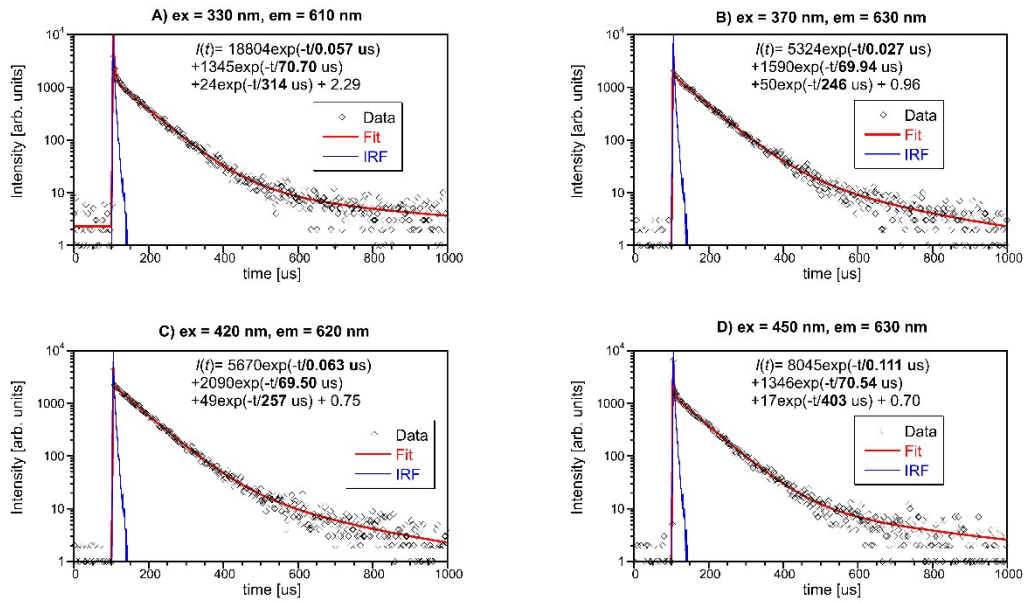


Fig. S6: PL decay curves for undoped Li_2MnCl_4 . Excitation and emission wavelengths are listed in the title of each subfigure. Red solid line is convolution of function $I(t)$ and instrumental response.

Tab. S3: Summary of the PL decay kinetics of undoped Li_2MnCl_4 . X_i is an integral contribution of i -th component.

λ_{ex} [nm]	$\lambda_{\text{em}} \sim 620$ nm				t_{mean} [μs]
	t_1 [μs]	X_1 [%]	t_2 [μs]	X_2 [%]	
330	70.7	92.7	314.0	7.3	88.6
370	69.9	90.0	246.0	10.0	87.5
420	69.5	92.0	257.0	8.0	84.5
450	70.5	93.3	403.0	6.7	92.9

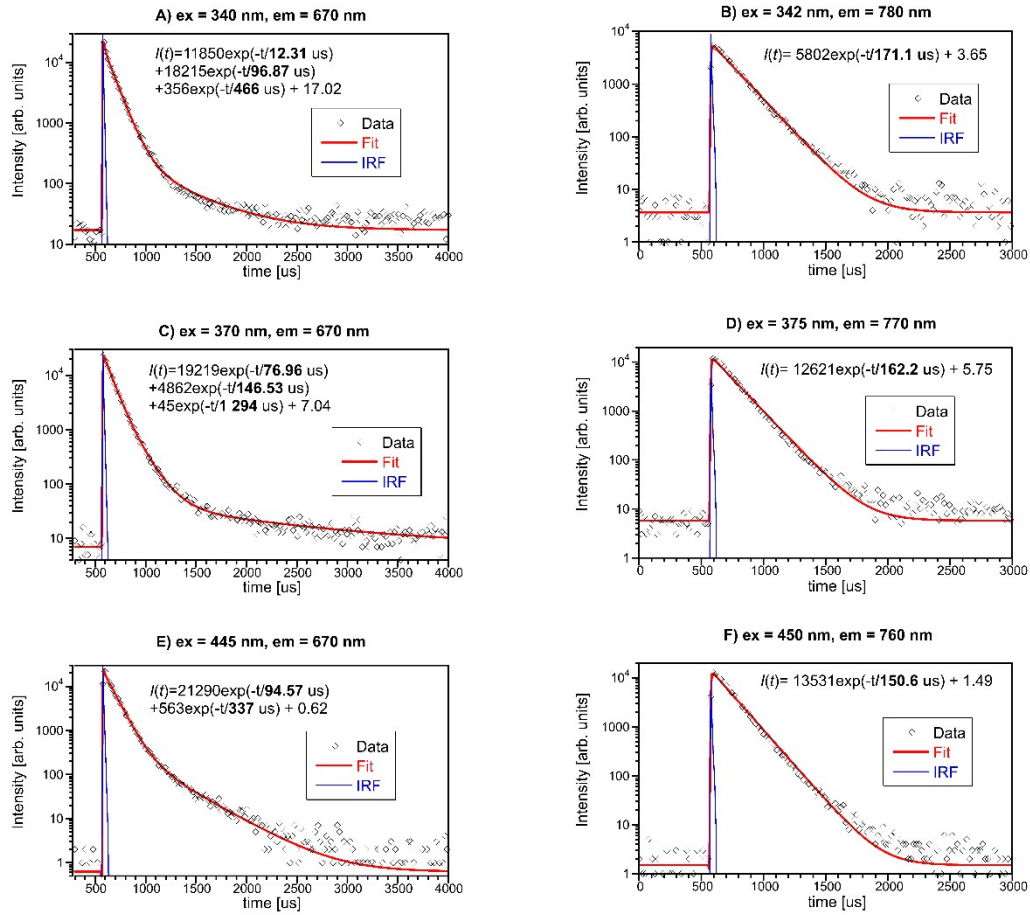


Fig. S7: PL decays of $\text{Li}_2\text{MnCl}_4:\text{Eu}$. Red solid line is convolution of function $I(t)$ and instrumental response.

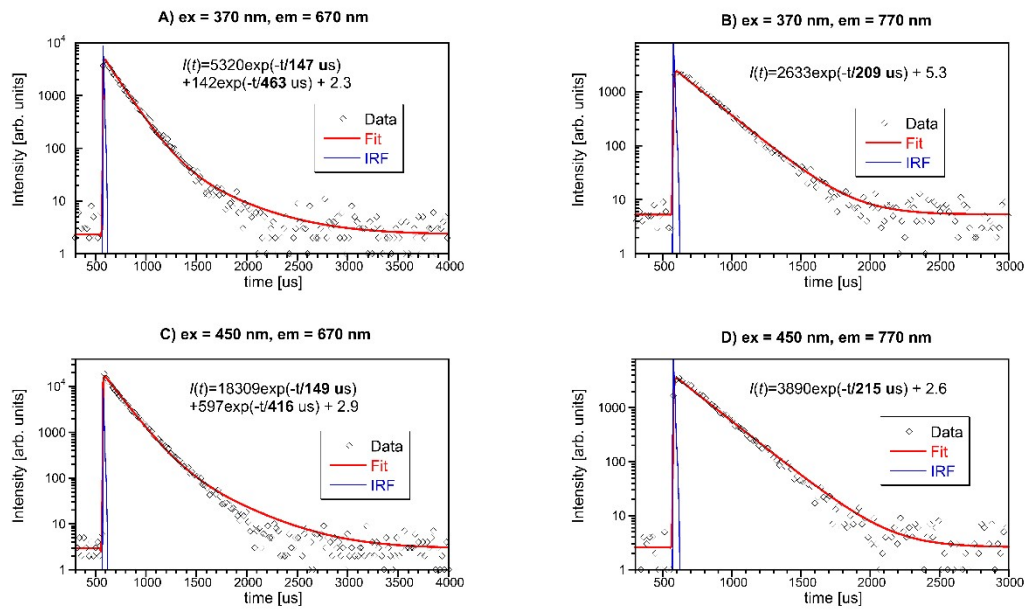


Fig. S8: PL decays of $\text{Li}_2\text{MnCl}_4:\text{Ce}$. Red solid line is convolution of function $I(t)$ and instrumental response.

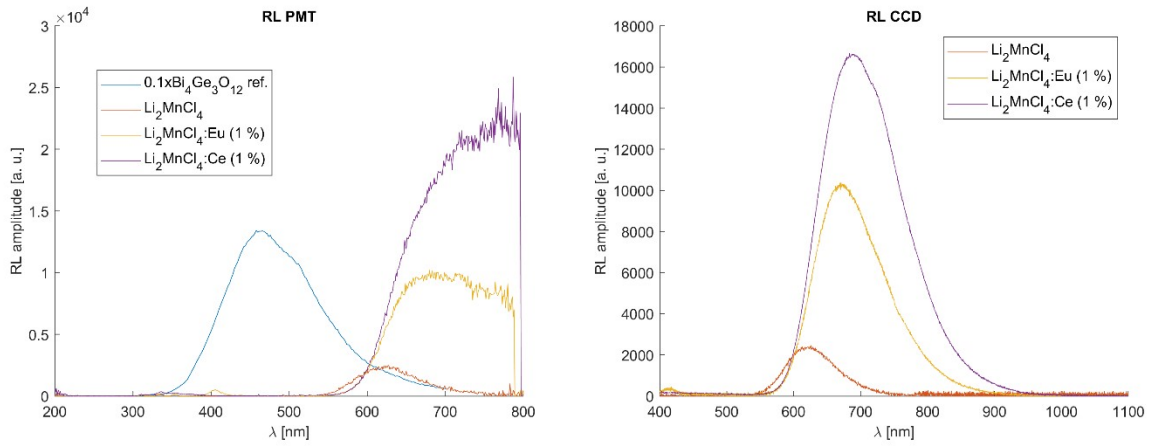


Fig. S9: RL spectra measured using PMT (left) and CCD (right) as photodetector.

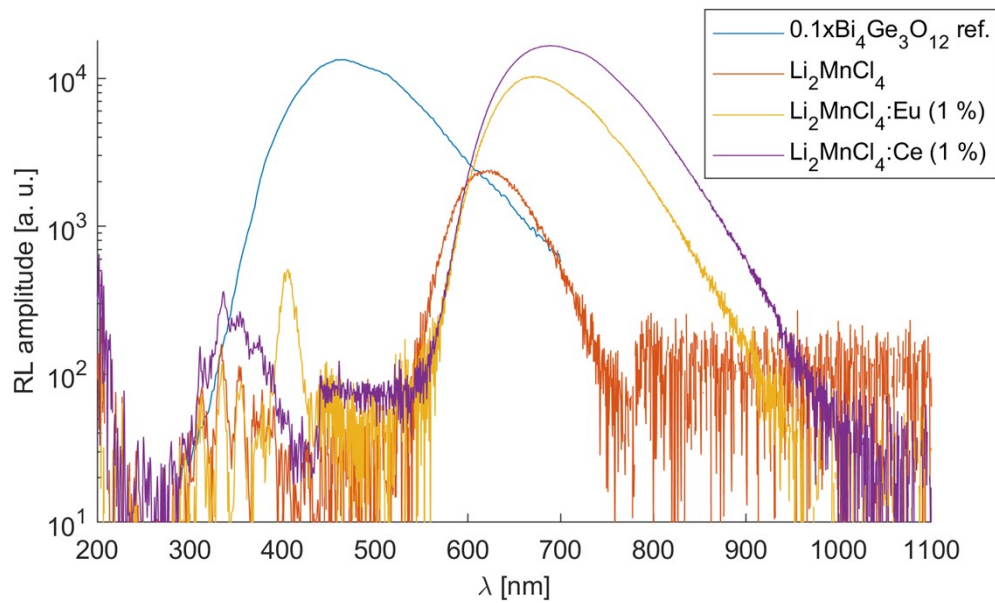


Figure S10: RL spectra of all three Li₂MnCl₄ samples together with BGO reference sample. The amplitude of BGO spectrum was divided by 10 for better comparison. The artefact in BGO spectrum near 800 nm is due to overcorrection.

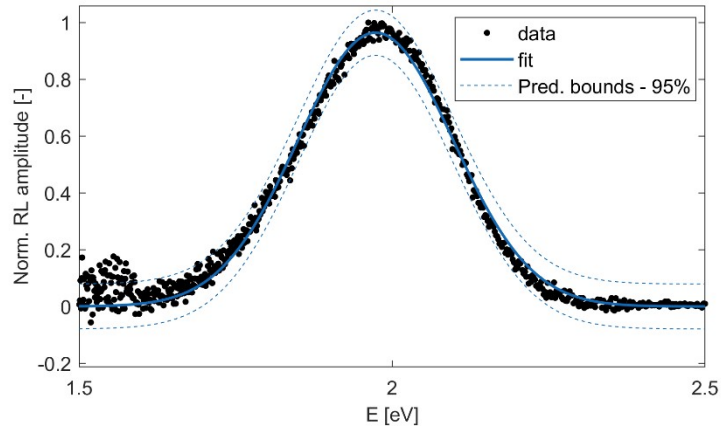


Fig. S11: Normalized RL spectra of undoped Li_2MnCl_4 approximated by a single gaussian function.

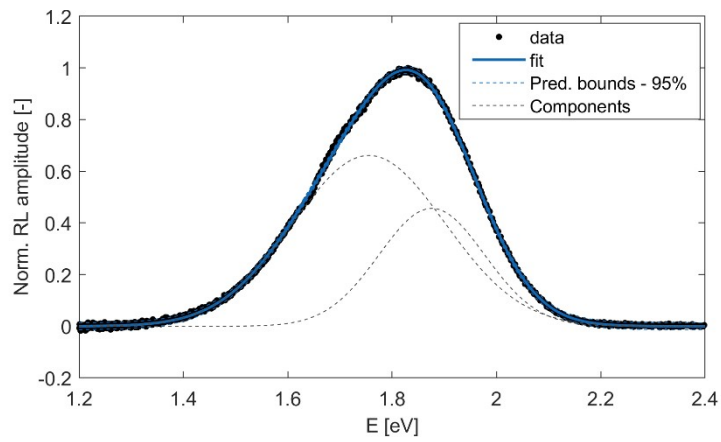


Fig. S12: Normalized RL spectra of $\text{Li}_2\text{MnCl}_4:\text{Eu}^{2+}$ approximated by a sum of two gaussian functions.

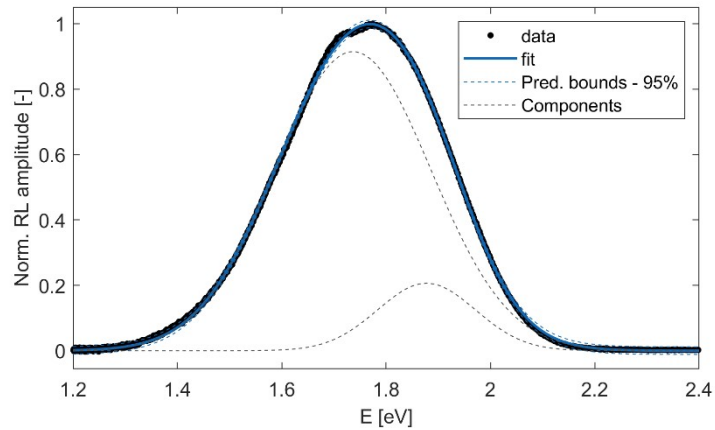


Fig. S13: Normalized RL spectra of $\text{Li}_2\text{MnCl}_4:\text{Ce}^{3+}$ approximated by a sum of two gaussian functions